The Cerebellum (2019) 18:298–308
https://doi.org/10.1007/s12311-018-0988-4

ORIGINAL PAPER

Abnormal Cerebellar Connectivity Patterns in Patients with Parkinson's Disease and Freezing of Gait

Komal Bharti[1] · Antonio Suppa[1,2] · Sara Pietracupa[2] · Neeraj Upadhyay[1] · Costanza Giannì[1] · Giorgio Leodori[2] · Francesca Di Biasio[3] · Nicola Modugno[2] · Nikolaos Petsas[2] · Giovanni Grillea[2] · Alessandro Zampogna[1] · Alfredo Berardelli[1,2] · Patrizia Pantano[1,2]

Published online: 3 November 2018

Abstract
In this study, we aimed to evaluate the importance of cerebellum in freezing of gait (FOG) pathophysiology. Due to the fundamental role of the cerebellum in posture and gait control, we examined cerebellar structural and functional connectivity (FC) in patients with PD and FOG. We recruited 15 PD with FOG (PD-FOG), 16 PD without FOG (PD-nFOG) patients, and 16 healthy subjects (HS). The FOG Questionnaire (FOG-Q) assessed FOG severity. Three tesla-MRI study included resting-state functional MRI, diffusion tensor imaging (DTI), and 3D T1-w images. We located seed regions in the cerebellar locomotor region, fastigial, and dentate nucleus to evaluate their FC. DTI parameters were obtained on the superior, middle, and inferior cerebellar peduncles. Global and lobular cerebellum volumes were also calculated. Cerebellar locomotor and fastigial FC was higher in cerebellar and posterior cortical areas in PD-FOG than in HS. FC of the cerebellar locomotor region with cerebellar areas positively correlated with FOG-Q. Dentate FC was lower in the prefrontal and parieto-occipital cortices in PD-FOG than in HS and in the brainstem, right basal ganglia, and frontal and parieto-occipital cortices than in PD-nFOG. DTI parameters in superior and middle cerebellar peduncles were altered in PD-FOG compared with PD-nFOG and significantly correlated with FOG-Q. There were no differences in cerebellar volumes between PD-FOG and either PD-nFOG or HS. Our results suggest that altered connectivity of the cerebellum contributes to the pathophysiology of FOG. FC of the cerebellar locomotor region and white matter (WM) properties of cerebellar peduncles correlate with FOG severity, supporting the hypothesis that abnormal cerebellar function underlies FOG in PD.

Keywords Resting-state functional magnetic resonance imaging · Functional connectivity · Parkinson's disease · Freezing of gait · Cerebellar locomotor region · Fastigial nucleus · Dentate nucleus

Introduction

Freezing of gait (FOG) is a disabling gait disturbance, characterized by the inability to initiate movement and maintain locomotion, that often occurs in patients with Parkinson's disease (PD) [1].

The pathophysiological mechanism underlying FOG in PD has yet to be fully understood. Studies based on magnetic resonance imaging (MRI) have reported various structural and functional abnormalities in the cortical and subcortical brain areas of PD patients with FOG (PD-FOG): abnormalities in frontal, parietal, and occipital cortical areas as well as disconnection between the cerebral cortex and subcortical structures have been hypothesized to play an important role in the pathogenesis of FOG [2–9]. Recent MRI data have suggested that the structural and functional disconnection between the cerebellum and other gray matter structures may play a key role in the FOG phenomenon [4, 5, 8]. Altered functional connectivity (FC) between the supplementary motor area (SMA) and the cerebellar locomotor region (CLR), a structure that regulates automatic posture/gait control, has been described in PD-FOG [5]. Moreover, the CLR disconnection has recently been considered

✉ Patrizia Pantano
patrizia.pantano@uniroma1.it

[1] Department of Human Neurosciences, Sapienza University of Rome, Viale dell'Università, 30, 00185 Rome, Italy

[2] IRCCS Neuromed, Pozzilli, IS, Italy

[3] Unit of Neurology, San Martino Policlinic Hospital IST, Genoa, Italy

to underlie various forms of non-PD-related lesion-induced FOG [4]. Other cerebellar nuclei may, however, also be involved in the pathophysiology of FOG. Multimodal inputs converge on the fastigial nucleus (FN), which coordinates postural responses during walking by sending integrated body information to posture- and gait-related areas in the brainstem and cerebral cortex [10]. Furthermore, the cerebellum is anatomically and functionally connected with a number of brainstem structures crucially involved in gait and balance control such as the pedunculopontine nucleus [11]. Lastly, cognitive processes contributing to posture/gait control are mediated by functional interactions between the neo-cerebellum and the cerebral cortex through the dentate nucleus (DN) [12].

We hypothesized that several cerebellar nuclei and white matter (WM) connections may be involved in the pathophysiology of FOG. To test this hypothesis, we investigated functional and structural connectivity of the cerebellum. In particular, cerebellar FC was investigated by analyzing resting-state functional MRI data using the whole brain, seed-to-voxel approach, which entails locating the seeds on the CLR, FN, and DN. We also investigated cerebellar structural integrity and connectivity by evaluating cerebellar volumes and WM properties along the superior, middle, and inferior cerebellar peduncles (SCP, MCP, and ICP, respectively). Lastly, we investigated possible relationships between cerebellar functional and structural connectivity and the severity of FOG.

Materials and Methods

Subjects

Fifteen PD patients with FOG (PD-FOG) (3 females; mean age, 71.0 ± 7.1 years) were included in this study. As control groups, we also studied 16 PD patients without FOG (PD-nFOG) (3 females; mean age, 66.3 ± 10.9)) and 16 healthy subjects (HS) with no history of neurological or psychiatric illnesses (10 females; mean age, 66.7 ± 7.6 years). Participants were recruited at the Department of Human Neuroscience, Sapienza University of Rome, Italy, and at IRCCS Neuromed Institute, Italy. The diagnosis of PD was based on standardized clinical criteria [13] and confirmed by follow-up clinical evaluations according to EFNS recommendations [14].

Exclusion criteria included atypical or secondary parkinsonisms, the coexistence of severe systemic diseases or other psychiatric or neurological illnesses as well as severe cognitive deficits, as indicated by a Mini-mental State Examination (MMSE) score of less than 26 [15]. Patients were clinically assessed by the Hoehn and Yahr scale (H&Y) [16] and the Unified Parkinson's disease rating scale part III (UPDRS-III) [17]. Frontal cognitive function was tested by Frontal Assessment Battery (FAB) [18], whereas depression was evaluated by Hamilton Depression Scale (HAM-D) [19]. The presence of FOG was evaluated by direct observation of a paroxysmal interruption of stride or marked reduction in forward feet progression [1] during a "Timed get Up and Go" (TUG) test (Mathias et al. 1986). The severity of FOG was assessed by the FOG Questionnaire (FOG-Q) [20], a reliable tool to investigate FOG [21, 22]. FOG-Q consists of 16 items assessing gait in daily living, frequency and severity of FOG, frequency of festinating gait and its relation to falls, and frequency and severity of falls. The total score consists of a 5-point scale where a score of 0 indicates absence of the symptom, while 4 indicates the most severe. All patients were evaluated 1 h after acute L-dopa administration (ON state) and after L-dopa withdrawal for at least 12 h (OFF state). Patients were clinically evaluated by neurologists expert in movement disorders. All patients underwent the MRI examination in a clinically defined OFF state. The study was conducted with institutional Ethics Committee approval and in accordance with the Declaration of Helsinki. Written informed consent was obtained from each participant.

Imaging Protocol

Functional and structural MRI data were acquired with a 3-tesla scanner (Magnetic Verio; Siemens, Erlangen, Germany) using a standardized protocol and a 12-channel head coil designed for parallel imaging (GRAPPA, generalized autocalibrating partially parallel acquisition). We acquired blood oxygenation level-dependent (BOLD) single-shot echo-planar images (TR = 3.00 ms, TE = 30 ms, flip angle = 89°, 64 × 64 matrix, 50 contiguous 3-mm-thick axial slices, 140 volumes, acquisition time = 7 min) in the resting condition; participants were instructed not to consume any tea or coffee or take other stimulants and not to have lunch for a minimum of 2 h before the scan. Participants were instructed to lie down straight in a fully awake and relaxed condition during the scan. We also acquired high-resolution 3D T1-weighted MPRAGE sequences (TR = 1900 ms, TE = 2.93 ms, 176 sagittal 1-mm-thick sections, without a gap, flip angle = 9°, FOV = 260 mm, matrix = 256 × 256) and diffusion tensor imaging (DTI) (single-shot echo-planar spin echo sequence with 30 directions, TR = 12,200 ms, TE = 94 ms, FOV = 192 mm, matrix = 96 × 96, $b = 0$ and 1000 s/mm^2, 72 axial 2-mm-thick slices, no gap). Lastly, standard dual turbo spin-echo (TR = 3320 ms, TE = 10/103 ms, FOV = 220 mm, matrix = 384 × 384, 25 axial 4-mm-thick slices, 30% gap) sequences were acquired to exclude patients with structural lesions.

Data Analysis

Resting-State Functional MRI Analysis

The data were analyzed using FSL (FMRIB software library package) (http://www.fmrib.ox.ac.uk/fsl).

Preprocessing

Single subject pre-processing and group analysis were performed using the fMRI Expert Analysis Tool (https://fsl.fmrib.ox.ac.uk/fsl/fslwiki) [23]. The pre-processing steps include brain extraction of T1-3D images, head motion correction, slice timing correction, and spatial smoothing using a Gaussian kernel of full width at half maximum of 5 mm and a high pass temporal filtering cutoff of 100 s. To perform high-level group comparisons, the FMRIB linear image registration tool (http://www.fmrib.ox.ac.uk/fsl) and non-linear image registration tool (https://fsl.fmrib.ox.ac.uk/fsl/fslwiki/FNIRT) were used to register functional images with the processed brain extracted images and Montreal Neurological Institute (MNI) standard space.

Seed Description (CLR, FN, and DN)

Individual seed ROI masks of the CLR, FN, and DN were obtained from high-resolution T1 images of individual subjects using FMRIB's Integrated Registration and Segmentation tool (https://fsl.fmrib.ox.ac.uk/fsl/fslwiki/FIRST), an automatic subcortical segmentation program. Three 2-mm radius spherical ROIs were created individually for each nucleus using coordinates reported in the literature (9,38,39): CLR (left: $x = -7$, $y = -52$, $z = -16$; right: $x = 7$, $y = -52$, $z = -16$), FN (left: $x = -3$, $y = -52$, $z = -28$; right: $x = 3$, $y = -52$, $z = -28$), and DN (left: $x = -17$, $y = -58$, $z = -35$; right: $x = 17$, $y = -56$, $z = -35$) on the standard MNI_2-mm template in the FSL Toolbox. Left and right ROIs of each of the CLR, FN, and DN were merged to obtain a single bilateral mask. Each mask was then transformed into the individual functional data space, by applying the combined linear and inverse non-linear deformation matrix, to extract the related average time course series. The time series were then fed into the fMRI Expert Analysis Tool to produce individual subject-level correlation maps for all the voxels (family-wise error [FWE], corrected at $p < 0.05$). The output was positively or negatively correlated with each of the seeds. Subject-level FC maps were entered in a group, high-level analysis using FMRIB'S Expert Analysis Tool (FEAT), part of FSL (fmrib.ox.ac.uk/fsl/fslwiki/FEAT). The mixed-effects, general linear model was applied to test the average of each group and between-group differences using a two-sample, unpaired t test. Results were transformed into Z statistic images and thresholded by using clusters determined by $Z > 2.3$, corrected for whole brain FWE approach using multiple comparisons and thresholded for cluster significance of $p < 0.05$. Further, since the PD-FOG group was compared against two different control groups, we applied Bonferroni's correction for multiple comparisons by a factor 2, so considering as significant $p < 0.025$ (for the lowest voxel in the z score map of value 2.3, the corresponding p value is 0.0215 for a two-tailed distribution). The Harvard-Oxford Cortical and Subcortical Structural Atlas and Probabilistic Cerebellar atlas, included in FSL, were used to determine the anatomic localization of significant clusters.

Nuisance Signal Regression and Covariates of No Interest Included in the Model

Considering the noise in the data, we first identified the seeds of cerebrospinal fluid and WM on individual functional echo-planar images [24, 25]. Their extracted time series were then added as covariates of no interest (nuisance) to remove the contributions of the non-neural BOLD signal and improve the data specificity. The age, gender, disease duration, and motion parameters of the participants were also inserted into the model as covariates of no interest.

DTI Analysis

Pre-processing

DTI Fit, a part of FMRIB's diffusion toolbox (http://fsl.fmrib.ox.ac.uk), was used to generate fractional anisotropy (FA) and mean diffusivity (MD) maps.

Tract-Based Spatial Statistical Analysis

First, FA maps were subjected to the Tract-Based Spatial Statistical (TBSS) tool (https://fsl.fmrib.ox.ac.uk/fsl/fslwiki) for the voxel-wise statistical analysis and then were aligned into a common space by using a non-linear image registration tool. As registration target, we opted for using the FMRIB58_FA_1-mm image, which is the recommended option in TBSS. This target was non-linearly registered with other FA maps, which were then transformed into MNI standard space. The obtained mean FA image was then thinned to create a mean FA skeleton, representing the common center of WM tracts. A threshold of 0.2 was used to create a mean FA skeleton, which includes major WM tracts and excludes peripheral tracts. Each subject's aligned FA maps were projected into the mean FA skeleton. The resulting FA maps were then fed into voxel-wise general modeling cross-subject statistics to make two-sample unpaired t tests with covariates of no interest (age, gender, disease duration, and motion parameters). A non-parametric test of 5000 random permutations was run, and a threshold-free cluster enhancement technique (TFCE) was applied [26]. Results were reported at multiple comparisons using the FWE correction approach at a significance level of $p < 0.05$. SCP, MCP, and ICP were selected as ROIs using the JHU ICBM-DTI-81 White-Matter atlas in FSL library. Further, MD data was analyzed using TBSS in a similar manner.

Cerebellar Volumetry Analysis

In order to calculate the cerebellar volumes on the T1-weighted MR images of the subgroups of PD patients and HS, we used the Spatially Unbiased Infratentorial toolbox (SUIT) version 3.2 implemented in SPM12 [27, 28].

To isolate the cerebellum and the corresponding cerebellar mask, T1 weighted MR images of the sub group of PD patients and HS were subjected to isolation and segmentation. The isolated cerebellar mask was visually verified for every subject and was corrected when necessary by manually eliminating non-cerebellar voxels or including erroneously excluded cerebellar voxels. The isolated cerebellum was further normalized to align the isolated cerebellum from the native subject space to the SUIT atlas template space using the affine transformation matrix and non-linear flow field. The cerebellum in the SUIT atlas space was resliced in order to preserve the volume of different cerebellar lobules. Lastly, the obtained SUIT atlas was realigned back to the native subject space. The lobular volumes of the cerebellum were calculated through "Lobuli-ROI analysis with atlas" and were computed as the sum of the hemispheres as well as vermis. Finally, global volume of the cerebellum, the anterior and posterior volume of the cerebellum, was calculated as sum of lobules I–V and VI–X. The lobular volumes of the PD patients and HS were compared using two-sample *t* test in SPSS software (SPSS Inc., Chicago, IL, USA). In order to evaluate possible gray matter volume differences in the three seed regions (CLR, FN, and DN), normalized MR images to SUIT space were used to perform voxel-based morphometry analysis inserting the seed region masks explicitly. A between-subject ANOVA was implemented to check possible between-group differences and explorative results (FWE, corrected at $p < 0.05$). We further applied small volume correction (SVC) in the three seed regions (CLR, FN, and DN) to investigate volume differences between the two subgroups of PD patients and between patients and HS (FWE, corrected at $p < 0.05$).

Clinico-Radiological Correlation

A correlation analysis was performed between the FC differences (CLR, FN, and DN) and the clinical scores, i.e., FOG-Q, UPDRS, MMSE, FAB, H&Y, and HAM-D, using a general linear model implemented in FSL with covariates of no interest (age, gender, disease duration, and motion parameters). Statistical differences were assessed within the mask of the FC differences of CLR, FN, and DN maps. A non-parametric test of 5000 random permutations was run, and a threshold-free cluster enhancement technique was applied. Lastly, the functional correlation results were corrected for multiple comparisons using the FWE correction approach at a significance level of $p < 0.05$.

Similarly, a correlation analysis was performed between the significant DTI differences in the FA and MD with the clinical scores, i.e., FOG-Q, UPDRS, MMSE, FAB, H&Y, and HAM-D using general linear model implemented in FSL with covariates of no interest (age, gender, disease duration, and motion parameters). Statistical differences were assessed to extract the related time course series by running 5000 non-parametric random permutations and a threshold-free cluster enhancement technique. Finally, we reported DTI correlation results corrected for multiple comparisons using the FWE correction approach at a significance level of $p < 0.05$.

Results

The demographic and clinical details of the patients are shown in Table 1. The Shapiro-Wilk Normality test was performed to check the normal distribution of the demographic and clinical scores. The demographic and clinical data of the two subgroups of PD patients were comparable in age, gender, disease duration, motion parameters, clinical scores, and gray matter volume of the seed regions (CLR, FN, and DN) (all $p > 0.05$). Voxel-based morphometry results showed no significant differences in the gray matter volume of CLR, FN, and DN seed regions between subgroups of PD patients and HS. Additionally, no statistically significant differences were observed even in the age between either the PD-FOG and HS ($p = 0.11$) or the PD-nFOG and HS ($p = 0.99$).

Functional Connectivity Results

Compared with HS, PD-FOG exhibited increased FC of the CLR in cerebellar areas (vermis, left hemispheric lobules VI, IX, right crus I and right hemispheric lobules I–IV, VI, VII a, and VII b) and in the parieto-occipital cortex (fusiform gyrus and lateral occipital cortex bilaterally and right lingual gyrus) (corrected for multiple comparisons, at FWE, $p < 0.025$) (Fig. 1). The increased FC between CLR was located in the cerebellar vermis, left hemispheric lobule IX, right crus I and right hemispheric lobules I–IV and VI positively correlated with FOG-Q (corrected for multiple comparisons, at FWE, $p < 0.05$) (Fig. 2). Similarly, the FC between the FN and the cerebellar vermis, left cerebellar lobule V, and left lateral occipital cortex was significantly higher in PD-FOG than in HS (corrected for multiple comparisons, at FWE, $p < 0.025$) (Fig. 3).

In both subgroups of PD patients, the FC of both the CLR and the FN with the prefrontal cortex (superior and middle frontal gyri and anterior cingulate cortex) was decreased bilaterally, with respect to HS (corrected for multiple corrections, at FWE, $p < 0.025$) (Figs. 1 and 3).

Table 1 Demographic and clinical characteristics of the PD patients

	PD-FOG ($n = 15$)	PD-nFOG ($n = 16$)	p value[a]
Age (years)	71.0 ± 7.1	66.3 ± 10.9	0.16
Male/female	12/3	13/3	0.92
Disease duration (years)	11 ± 6.2	8.6 ± 5.3	0.25
UPDRS-III	36.2 ± 12.1	29 ± 17.4	0.19
H&Y	2.3 ± 0.7	2 ± 0.8	0.27
MMSE	28.5 ± 1.8	27.5 ± 1.9	0.14
FAB	14.7 ± 2.4	14.8 ± 2.1	0.90

PD-FOG, Parkinson's disease with freezing of gait; *PD-nFOG*, Parkinson's disease with no freezing of gait; *UPDRS-III*, Unified Parkinson's Disease Rating Scale OFF and ON therapy; *H&Y*, Hoehn and Yahr scale; *MMSE*, Mini-Mental State Examination; *FAB*, Frontal Assessment Battery. *FOG-Q*, FOG questionnaire. Values are reported as mean ± SD

[a] Differences between the demographic and clinical scores of PD-FOG and PD-nFOG were assessed by t test, except for gender (χ^2 test)

Lastly, the FC of the DN was altered only in PD-FOG, who displayed decreased FC with the prefrontal (superior and middle frontal gyri bilaterally and right anterior cingulate cortex) and parieto-occipital cortices (lateral occipital cortex and inferior parietal lobule, bilaterally) than HS. Moreover, PD-FOG exhibited decreased FC between the DN and several brain areas (brainstem, right pallidum and putamen, orbitofrontal

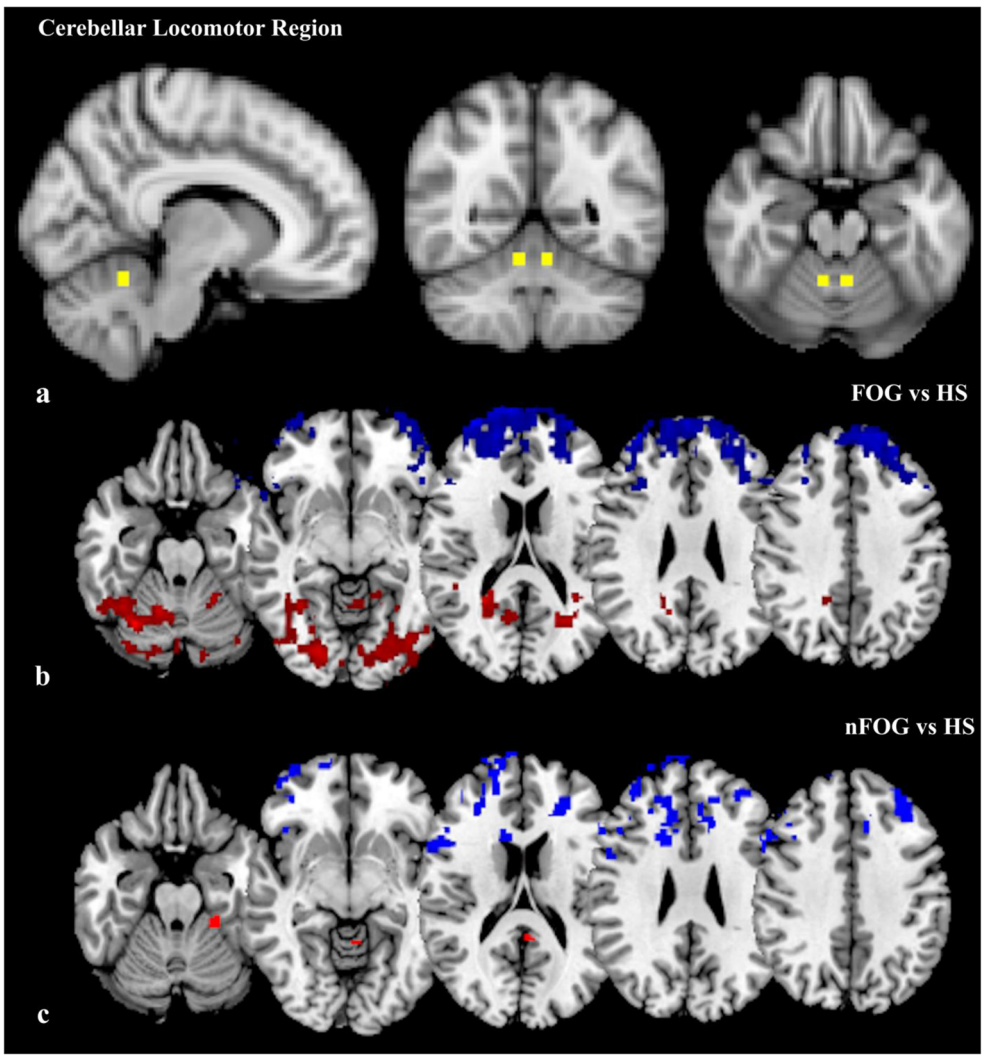

Fig. 1 rsFC differences between the sub-groups of PD patients and healthy subjects (HS) obtained from the cerebellar locomotor region (CLR) (two-sample t test; family-wise error (FWE), corrected at $p < 0.025$). **a** seed map of the CLR. **b** FC differences between PD patients with FOG (PD-FOG) and HS. **c** FC differences between PD patients with no FOG (PD-nFOG) and HS. Red: increased CLR connectivity. Blue: decreased CLR connectivity. Results are corrected for multiple comparisons at FWE, $p < 0.025$. Images are shown according to radiologic orientation

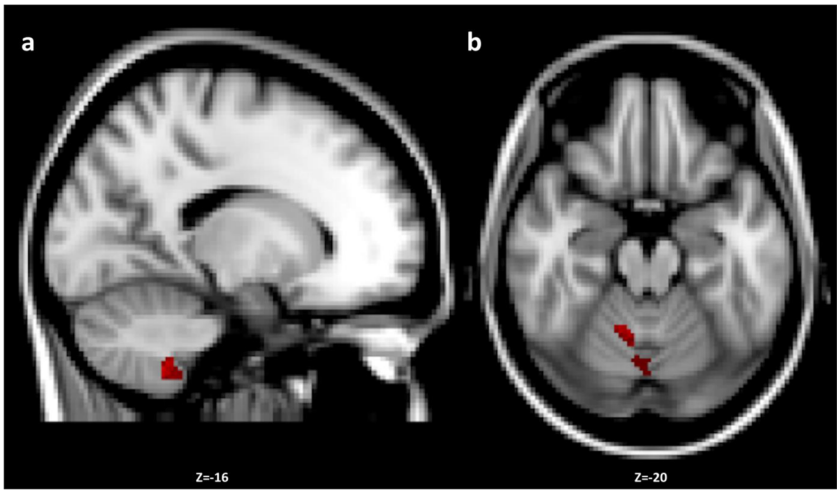

Fig. 2 Correlation of the CLR functional connectivity with the severity of FOG (FOG-Q) (family-wise error (FWE), corrected at $p < 0.05$). Areas of positive correlation (red) were located in the cerebellar vermis, left lobule IX, right crus I, and right lobules I–IV and VI. Results were obtained within the mask of FC differences between PD-FOG patients and HS and were corrected for multiple comparisons at FWE, $p < 0.05$

cortex bilaterally, left prefrontal cortex, precuneus, and calcarine cortex, bilaterally) with respect to PD-nFOG (corrected for multiple comparisons, at FWE, $p < 0.025$) (Fig. 4).

Besides the significant correlation between the FC of the CLR and FOG severity, no other significant correlation were found between the cerebellar nuclei FC and other clinical measures.

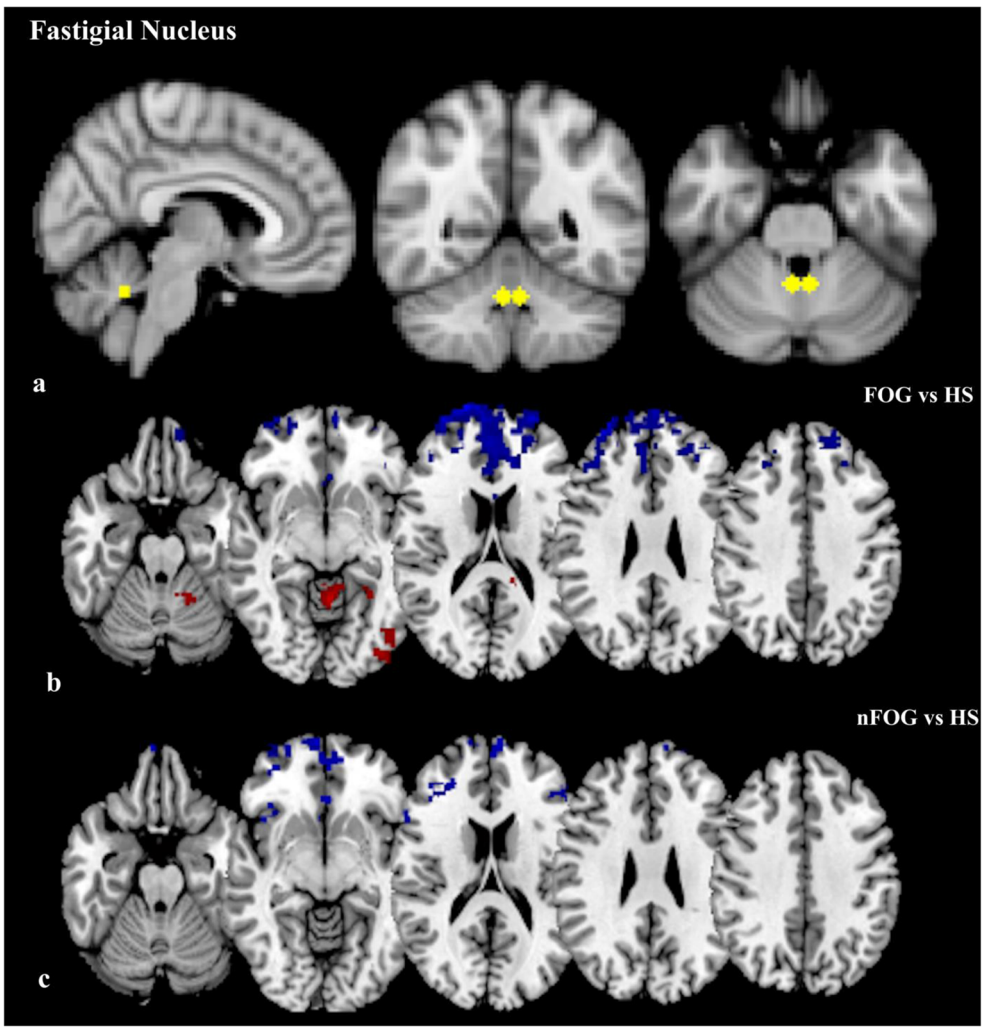

Fig. 3 rsFC differences between the subgroups of PD patients and healthy subjects (HS) obtained from the fastigial nucleus (FN) (two-sample *t* test, family-wise error (FWE), corrected at $p < 0.025$). a: seed map of the FN. b: FC differences between PD patients with FOG (PD-FOG) and HS. c: FC differences between PD patients with no FOG (PD-nFOG) and HS**.** Red: increased FN connectivity. Blue: decreased FN connectivity. Results are corrected for multiple comparisons at FWE, $p < 0.025$. Images are shown according to radiologic orientation

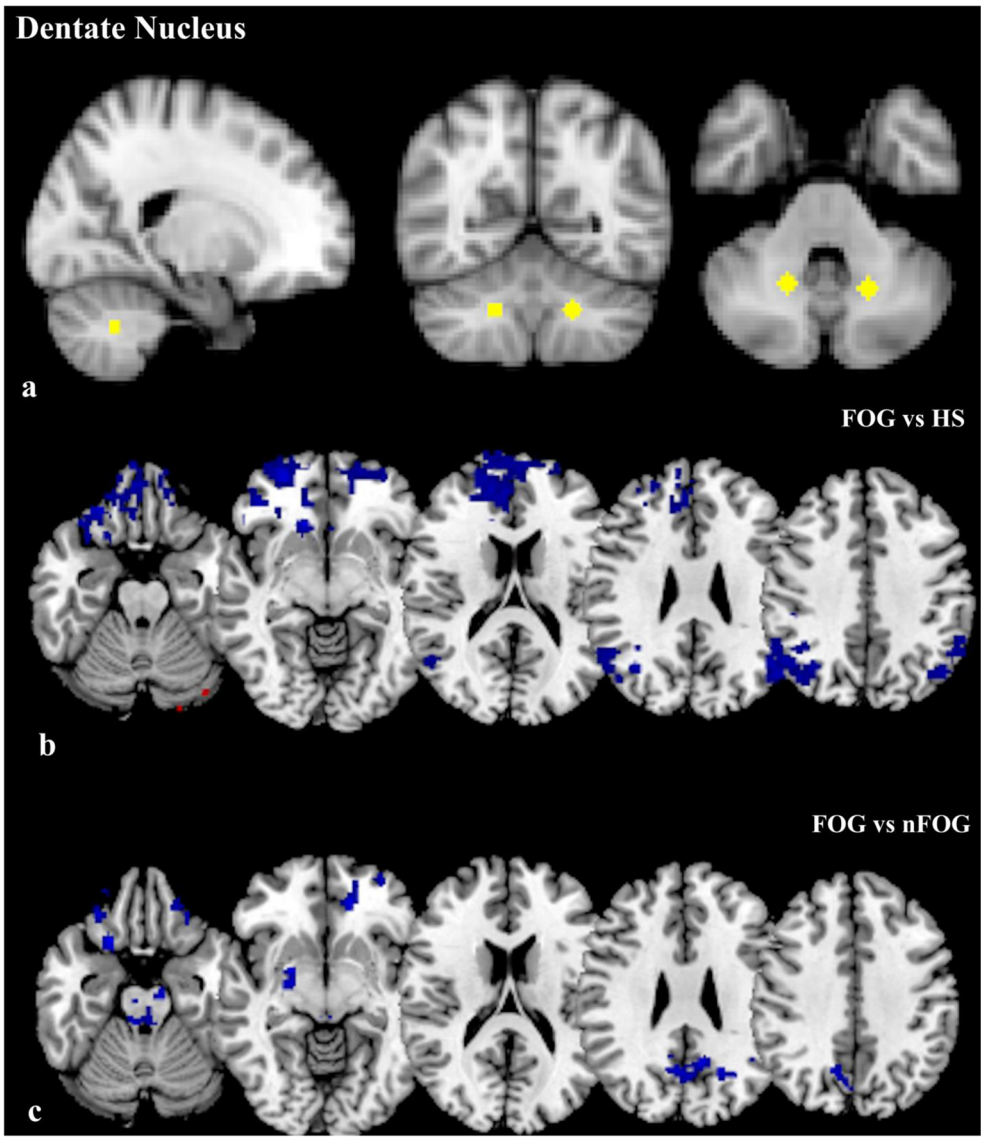

Fig. 4 rsFC differences between subgroups of PD patients and healthy subjects (HS) obtained from the dentate nucleus (DN) (two-sample *t* test, family-wise error (FWE), corrected at $p < 0.025$). **a** seed map of the DN. **b** FC differences between PD patients with FOG (PD-FOG) and HS. **c** FC differences between PD-FOG and PD patients with no FOG (PD-nFOG). Red: increased DN connectivity. Blue: decreased DN connectivity. Results were corrected for multiple comparisons at FWE, $p < 0.025$. Images are shown according to radiologic orientation

DTI Results

The PD-FOG exhibited lower FA values in the SCP and MCP than PD-nFOG or HS. PD-FOG also displayed higher MD values in the SCP than PD-nFOG (corrected for multiple comparisons, at FWE, $p < 0.05$) (Fig. 5).

In PD-FOG, FA values in the MCP and SCP negatively correlated with FOG-Q scores while MD values in the SCP positively correlated with FOG-Q scores (corrected for multiple comparisons, at FWE, $p < 0.05$) (Fig. 6). No other significant correlations were found between cerebellar DTI parameters and other clinical measures.

Cerebellar Volumetric Results

Global cerebellar volumes were 91.23 ± 28.61 milliliter (mL) in PD-FOG, 93.67 ± 33.02 mL in PD-nFOG patients and 89.07 ± 26.28 mL in HS. We did not find global or lobular cerebellar volume differences between PD-FOG and the two control groups (PD-nFOG and HS) (all $p > 0.05$).

Discussion

In this study, we combined advanced MRI methods in order to investigate structural and functional alterations that potentially involve the cerebellum in PD-FOG. To this purpose, we evaluated the FC between three cerebellar structures, namely the CLR, FN, and DN, and the remaining cortical and subcortical brain regions as well as cerebellar volume and fiber integrity along the three cerebellar peduncles. When compared with HS, PD-FOG exhibited greater FC alterations than PD-nFOG. Interestingly, the increased FC between the CLR and some regions of the cerebellum correlated with FOG-Q scores

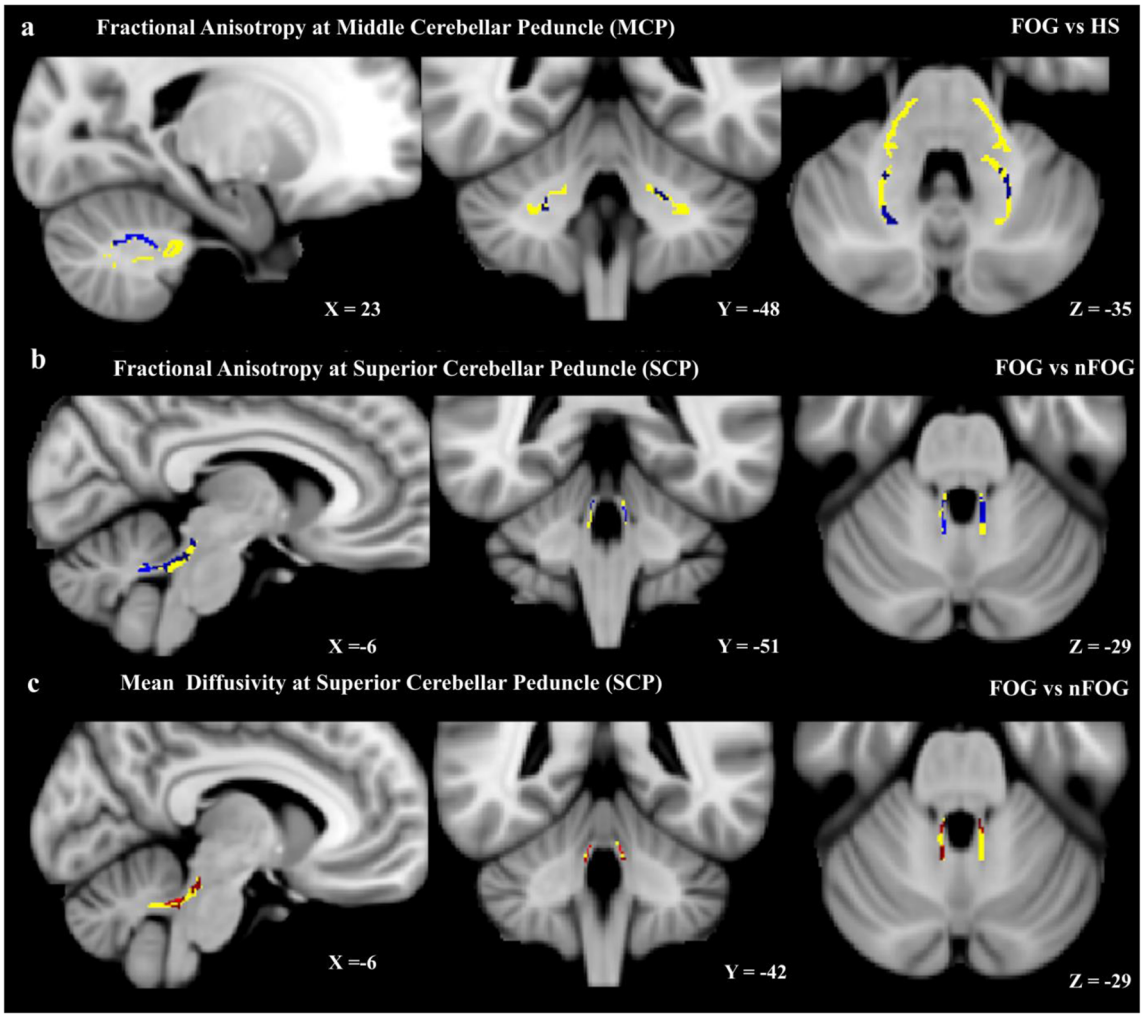

Fig. 5 Differences of mean diffusivity (MD) and fractional anisotropy (FA) between the subgroups of PD patients and healthy subjects (HS). **a** FA differences in the middle cerebellar peduncle (MCP) between PD-FOG and HS. **b** FA differences in the superior cerebellar peduncle (SCP) between patients with FOG (PD-FOG) and patients with no FOG (PD-nFOG). **c** MD differences in the SCP between PD-FOG and PD-nFOG. Red: increased MD and blue: decreased FA. Yellow: the maps of SCP and MCP. Results are corrected for multiple comparisons at FWE, $p < 0.05$. Images are shown according to radiologic orientation

suggesting that the functional disruption of this region not only plays an important role in the pathophysiology of FOG in PD, but also related to FOG severity. Moreover, the direct comparison between the two PD subgroups demonstrated lower FC of the DN with the brainstem, right basal ganglia, and frontal and parieto-occipital cortices in PD-FOG. These findings point to abnormalities in FC of these cerebellar structures as relevant pathophysiological mechanisms underlying FOG in PD. Consistent with FC abnormalities, we observed, despite normal cerebellar volumes, prominent ultrastructural damage of the fiber tracts passing through the SCP and MCP in PD-FOG, which lends further support to the hypothesized role of cerebellar disconnection in FOG.

In patients with PD-FOG the FC of both the CLR and FN with posterior cortical areas, i.e., cerebellar hemispheres, vermis, and parieto-occipital cortex resulted to be increased. Experimental evidences point to the importance of the CLR in gait control since stimulation of CLR induces locomotion in experimental animals [29]. In humans, Fling et al. (2014) described increased FC between the SMA and both the mesencephalic and cerebellar locomotor regions, in PD-FOG, which points to functional reorganization within the locomotor network [5]. More recently, when Fasano et al. (2017) mapped lesions causing FOG in a common brain atlas, they observed heterogeneous brain lesions, but shared FC between these lesions and a focal area in the dorsal medial cerebellum corresponding to the CLR [4]. However, the significant correlation between CLR FC changes in PD-FOG and the severity of FOG does not provide a causal relation; our finding points to the involvement of CLR in the pathophysiology of FOG. Our study provides additional information by suggesting a role of abnormal FC between the FN and posterior brain areas in FOG occurrence. By projecting to both motor and non-motor cortical areas, the FN provides real-time modulation

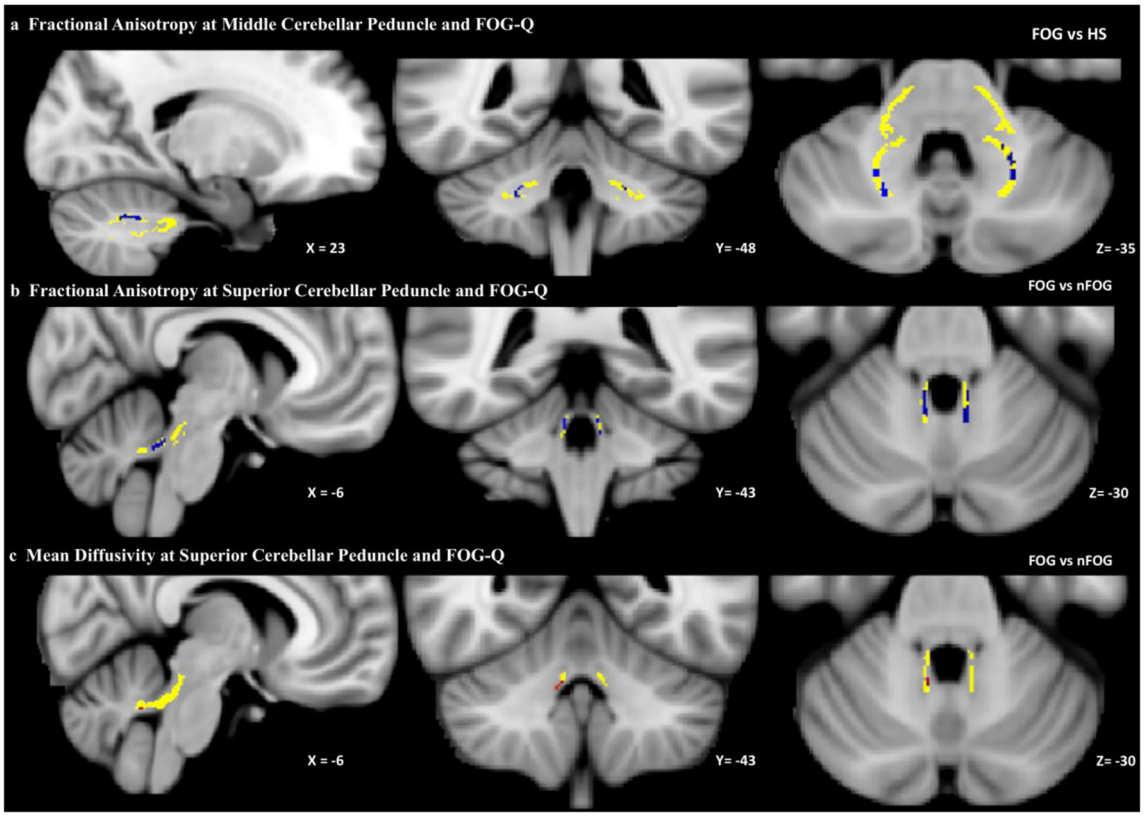

Fig. 6 Correlations of the DTI abnormalities with the severity of clinical symptoms. **a** correlation between fractional anisotropy (FA) at the middle cerebellar peduncle (MCP) and severity of freezing of gait (FOG-Q). **b** Correlation between fractional anisotropy (FA) at the superior cerebellar peduncle (SCP) and severity of freezing of gait (FOG-Q). **c** Correlation between the mean diffusivity (MD) at the superior cerebellar peduncle (SCP) and FOG-Q. Blue: negative correlation. Red: positive correlation. Results are corrected for multiple comparisons at FWE, $p < 0.05$. Images are shown according to radiologic orientation

of gait in relation to environmental changes [30]. Hence, the abnormal FC in the FN may alter the processing of multimodal inputs regarding postural stability during walking in PD-FOG. The abnormal FC between these two cerebellar regions and posterior cortical areas subserving visuo-spatial functions [3, 31] and areas of the anterior and posterior cerebellar lobes, which subserve motor and cognitive functions [32], support their role in FOG occurrence. The functional involvement of posterior associative cortex has been reported by other authors who analyzed functional MRI data by using the ICA. Tessitore et al. (2012) reported an association between reduced FC within the executive attention and visual networks in the right hemisphere and the severity of FOG [7]. Canu et al. (2015) reported reduced FC within the sensorimotor, default mode, and visual networks in PD-FOG [6].

FC in the DN was altered only in PD-FOG, in whom FC between the DN and the prefrontal and parieto-occipital cortices bilaterally was lower than in HS. The involvement of the DN is further supported by the direct comparison between PD-FOG and PD-nFOG, which showed lower FC between the DN and several brain regions (brainstem, right deep gray nuclei, and frontal and parieto-occipital cortices) in PD-FOG. This finding suggests reduced functional connectivity of the cerebellum with the neocortex, by both the cerebello-thalamo-cortical and the cortical-ponto-cerebellar loops, possibly contributing to postural and cognitive impairment [32–34] in PD-FOG.

Consistently, WM abnormalities, i.e., reduced FA values in the SCP and MCP and increased MD values in the SCP in PD-FOG, indicate cerebellar structural disconnection in FOG due to loss and/or damage of WM fibers connecting the cerebellum with supratentorial brain structures. Vice versa, the observation of normal DTI parameters in the ICP suggests the integrity of the dorsal spino-cerebellar pathways that project to the cerebellar cortex. Moreover, the significant correlations between axonal damage in the SCP and MCP and the severity of FOG further suggest that the cerebellum plays a role in the pathogenesis of FOG. Previous studies investigating DTI abnormalities in PD-FOG reported various WM abnormalities, mainly involving the pedunculopontine tract, corpus callosum, corticospinal tract, cerebral peduncles, cingulum, and superior and inferior longitudinal fasciculus [6, 9, 35], but not the cerebellar peduncles.

The strength of the study arises from our multimodal experimental approach (brain structural and functional by means of resting-state fMRI, DTI, and cerebellum-restricted VBM-

SUIT) in patients with PD, with and without FOG. Our findings overall have demonstrated that FOG is associated with abnormal structural and functional cerebellar connectivity. In addition, those structural and functional abnormalities significantly correlated with FOG severity (FOG-Q scores), a finding which points towards the involvement of cerebellar pathways in the pathophysiology of FOG in PD. Possible limitations of the study include the relatively small sample size of patients with and without FOG which might have contributed to the absence of significant changes in the direct comparison between PD-FOG and PD-nFOG.

In conclusion, we have here assessed FC not only in the CLR but also in other cerebellar nuclei, i.e., the FN and DN, together with ultrastructural DTI measures of cerebellar peduncles, in PD-FOG. Overall, our results suggest that abnormal cerebellar functional connectivity associated with microstructural disruption involving the SCP and MCP may contribute to the pathophysiology of FOG, despite preserved cerebellar GM volume.

Author Contribution KB, AS, SP, NU, CG, GL, FDB, NM, NP, GG, and AZ: patient recruitment, patient data collection, patient clinical and neuroradiological evaluation, data analysis, and manuscript preparation.

AB, PP: patient recruitment, patient data collection, patient clinical and neuroradiological evaluation, data analysis, manuscript preparation, critical revision of the manuscript.

Compliance with Ethical Standards

Conflict of Interest The authors declare that they have no conflict of interest.

Ethics Approval The study approved by our institutional review board and conformed with the declaration of Helsinki. All participants gave their written informed consent.

Publisher's Note Springer Nature remains neutral with regard to jurisdictional claims in published maps and institutional affiliations.

References

1. Nutt JG, Bloem BR, Giladi N, Hallett M, Horak FB, Nieuwboer A. Freezing of gait: moving forward on a mysterious clinical phenomenon. Lancet Neurol. 2011 [cited 2018 Feb 8];10:734–44. Available from: http://www.sciencedirect.com/science/article/pii/S1474442211701430.
2. Kostic VS, Agosta F, Pievani M, Stefanova E, Jecmenica-Lukic M, Scarale A, et al. Pattern of brain tissue loss associated with freezing of gait in Parkinson disease. Neurology. 2012;78:409–16.
3. Fasano A, Herman T, Tessitore A, Strafella AP, Bohnen NI. Neuroimaging of freezing of gait. J Park Dis. 2015;5:241–54.
4. Fasano A, Laganiere SE, Lam S, Fox MD. Lesions causing freezing of gait localize to a cerebellar functional network. Ann Neurol. 2017;81:129–41.
5. Fling BW, Cohen RG, Mancini M, Carpenter SD, Fair DA, Nutt JG, et al. Functional reorganization of the locomotor network in Parkinson patients with freezing of gait. PLoS One. 2014;9:e100291.
6. Canu E, Agosta F, Sarasso E, Volontè MA, Basaia S, Stojkovic T, et al. Brain structural and functional connectivity in Parkinson's disease with freezing of gait. Hum Brain Mapp. 2015;36:5064–78.
7. Tessitore A, Amboni M, Esposito F, Russo A, Picillo M, Marcuccio L, et al. Resting-state brain connectivity in patients with Parkinson's disease and freezing of gait. Parkinsonism Relat Disord. 2012 [cited 2016 Feb 18];18:781–7. Available from: http://www.sciencedirect.com/science/article/pii/S1353802012001228.
8. Wang M, Jiang S, Yuan Y, Zhang L, Ding J, Wang J, et al. Alterations of functional and structural connectivity of freezing of gait in Parkinson's disease. J Neurol. 2016 [cited 2017 Oct 10];263:1583–92. Available from: https://doi.org/10.1007/s00415-016-8174-4
9. Pietracupa S, Suppa A, Upadhyay N, Giannì C, Grillea G, Leodori G, et al. Freezing of gait in Parkinson's disease: gray and white matter abnormalities. J Neurol. 2018 [cited 2018 Feb 8];265:52–62. Available from: https://doi.org/10.1007/s00415-017-8654-1
10. Cavdar S, Onat FY, Yananli HR, Sehirli US, Tulay C, Saka E, et al. Cerebellar connections to the rostral reticular nucleus of the thalamus in the rat. J Anat. 2002;201:485–91.
11. Youn J, Lee J-M, Kwon H, Kim JS, Son TO, Cho JW. Alterations of mean diffusivity of pedunculopontine nucleus pathway in Parkinson's disease patients with freezing of gait. Parkinsonism Relat Disord. 2015;21:12–7.
12. Bostan AC, Dum RP, Strick PL. Cerebellar networks with the cerebral cortex and basal ganglia. Trends Cogn Sci. 2013 [cited 2017 Sep 25];17:241–54. Available from: http://www.sciencedirect.com/science/article/pii/S136466131300065X.
13. Postuma RB, Berg D, Stern M, Poewe W, Olanow CW, Oertel W, et al. MDS clinical diagnostic criteria for Parkinson's disease. Mov Disord. 2015;30:1591–601.
14. Berardelli A, Wenning GK, Antonini A, Berg D, Bloem BR, Bonifati V, et al. EFNS/MDS-ES/ENS [corrected] recommendations for the diagnosis of Parkinson's disease. Eur J Neurol. 2013;20:16–34.
15. Folstein MF, Folstein SE, McHugh PR. "Mini-mental state": a practical method for grading the cognitive state of patients for the clinician. J Psychiatr Res. 1975 [cited 2016 Mar 3];12:189–98. Available from: http://www.sciencedirect.com/science/article/pii/0022395675900266.
16. Hoehn MM, Yahr MD. Parkinsonism: onset, progression and mortality. Neurology. 1967;17:427–42.
17. Angelo Antonini GA. Validation of the Italian version of the Movement Disorder Society-Unified Parkinson's Disease Rating Scale. Neurol Sci. 2012;34.
18. Dubois B, Slachevsky A, Litvan I, Pillon B. The FAB: a frontal assessment battery at bedside. Neurology. 2000;55:1621–6.
19. Hamilton M. Comparative value of rating scales. Br J Clin Pharmacol. 1976 [cited 2017 May 22];3:58–60. Available from: https://doi.org/10.1111/j.1365-2125.1976.tb03714.x/abstract.
20. Giladi N, Shabtai H, Simon ES, Biran S, Tal J, Korczyn AD. Construction of freezing of gait questionnaire for patients with Parkinsonism. Parkinsonism Relat Disord. 2000 [cited 2017 Jul 26];6:165–70. Available from: http://www.sciencedirect.com/science/article/pii/S1353802099000620.
21. Giladi N, Tal J, Azulay T, Rascol O, Brooks DJ, Melamed E, et al. Validation of the freezing of gait questionnaire in patients with Parkinson's disease. Mov Disord. 2009;24:655–61.
22. Tambasco N, Simoni S, Eusebi P, Ripandelli F, Brahimi E, Sacchini E, et al. The validation of an Italian version of the Freezing of Gait Questionnaire. Neurol Sci. 2015;36:759–64.
23. Jenkinson M, Bannister P, Brady M, Smith S. Improved optimization for the robust and accurate linear registration and motion correction of brain images. NeuroImage. 2002;17:825–41.
24. Gavrilescu M, Shaw ME, Stuart GW, Eckersley P, Svalbe ID, Egan GF. Simulation of the effects of global normalization procedures in

functional MRI. NeuroImage. 2002 [cited 2017 Sep 12];17:532–42. Available from: http://www.sciencedirect.com/science/article/pii/S1053811902912267.
25. Macey PM, Macey KE, Kumar R, Harper RM. A method for removal of global effects from fMRI time series. NeuroImage. 2004;22:360–6.
26. Smith SM, Nichols TE. Threshold-free cluster enhancement: addressing problems of smoothing, threshold dependence and localisation in cluster inference. Neuroimage. 2009 [cited 2016 Mar 1];44:83–98. Available from: http://www.sciencedirect.com/science/article/pii/S1053811908002978.
27. Diedrichsen J, Balsters JH, Flavell J, Cussans E, Ramnani N. A probabilistic MR atlas of the human cerebellum. NeuroImage. 2009;46:39–46.
28. Diedrichsen J, Maderwald S, Küper M, Thürling M, Rabe K, Gizewski ER, et al. Imaging the deep cerebellar nuclei: a probabilistic atlas and normalization procedure. NeuroImage. 2011;54:1786–94.
29. Mori S, Matsui T, Kuze B, Asanome M, Nakajima K, Matsuyama K. Cerebellar-induced locomotion: reticulospinal control of spinal rhythm generating mechanism in cats. Ann N Y Acad Sci. 1998;860:94–105.
30. Takahashi R, Ishii K, Kakigi T, Yokoyama K, Mori E, Murakami T. Brain Alterations and Mini-Mental State Examination in patients with progressive supranuclear palsy: voxel-based investigations using 18F-fluorodeoxyglucose positron emission tomography and magnetic resonance imaging. Dement Geriatr Cogn Disord EXTRA. 2011 [cited 2017 Jan 19];1:381–92. Available from: http://www.ncbi.nlm.nih.gov/pmc/articles/PMC3243642/.
31. Botez MI, Botez T, Elie R, Attig E. Role of the cerebellum in complex human behavior. Ital J Neurol Sci. 1989;10:291–300.
32. Buckner RL. The cerebellum and cognitive function: 25 years of insight from anatomy and neuroimaging. Neuron. 2013;80:807–15.
33. Giladi N. Gait and mental function: the interplay between walking, behavior and cognition. J Neural Transm Vienna Austria 1996. 2007;114:1241–2.
34. Amboni M, Cozzolino A, Longo K, Picillo M, Barone P. Freezing of gait and executive functions in patients with Parkinson's disease. Mov Disord. 2008;23:395–400.
35. Vercruysse S, Leunissen I, Vervoort G, Vandenberghe W, Swinnen S, Nieuwboer A. Microstructural changes in white matter associated with freezing of gait in Parkinson's disease. Mov Disord. 2015 [cited 2017 Jan 30];30:567–76. Available from: https://doi.org/10.1002/mds.26130/abstract.